



UNIVERSIDAD NACIONAL DE COLOMBIA

# Integración de un modelo de la conectividad de los núcleos de la base del cerebro con información estructural para mejorar la detección de la RND en IRMF alteradas debido a ruido por movimiento

Aura María Forero Pachón

Universidad Nacional de Colombia  
Facultad de Medicina  
Bogotá, Colombia  
2017



# Integration of a connectivity model of the basal ganglia nuclei with structural information in order to enhance the default mode network detection in rs-fMRI corrupted by movement

Aura María Forero Pachón

Tesis presentada como requisito parcial para optar al título de:  
**Magister en Ingeniería Biomédica**

Director:  
Ph.D., Doctor. Eduardo Romero

Línea de Investigación:  
Imágenes Médicas  
Grupo de Investigación:  
Computer Imaging and Medical Applications Laboratory(Cimalab)

Universidad Nacional de Colombia  
Facultad de Medicina  
Bogota, Colombia  
2017

To family and friends who have accompanied  
and encourage me with love, patience and  
affection.

# Acknowledgment

This work was possible thanks to professor Eduardo Romero leader of CIMALAB research group, director of the Biomedical Engineering Master Program and of the Telemedicine center at Universidad Nacional de Colombia. He was the advisor of this work and without his guidance, advices, support and motivation it would not be possible.

Another special acknowledgment is for Norberto Malpica and Eva Manzanedo from LAIM-BIO at Universidad Rey Juan Carlos III, Spain, who gave very friendly assistance taking and sharing the images from the 14 people used in this study as well as the initial orientations at the beginning of this project.

# Abstract

This document presents a proposal devoted to improve the detection of the default mode network (DMN) in functional magnetic resonance imaging in noisy conditions caused by head movement. The proposed approach is inspired by the hierarchical treatment of information, in particular at the level of the brain basal ganglia. Essentially, the fact that information must be selected and reduced suggests propagation of information in the Central Nervous System (CNS) is anisotropic. Under this hypothesis, the reconstruction of information of activation should follow an anisotropic pattern. In this work, a diffusion anisotropic filter is used to recover a DMN that is perturbed by a certain degree of motion. Results obtained show this approach outperforms the state-of-the-art methods by 5.93%.

**Keywords:** Default mode network detection, rs-fMRI, artifacts caused by head motion, anisotropy, information flow, basal ganglia

# Resumen

%.

**Palabras clave:** Detección de la red neuronal por defecto, rs-fMRI, artefactos causados por movimiento de cabeza, anisotropía, flujo de información, núcleos de la base del cerebro.

# Figure List

1-1. Resting State Networks . . . . .	3
1-2. Default Mode Network. . . . .	4
1-3. Diagram representative of column neocortex. . . . .	6
1-4. Head motion . . . . .	8
2-1. Basal Ganglia. . . . .	12
2-2. Histology of the basal ganglia. . . . .	13
2-3. Information's flow in the Basal Ganglia. . . . .	13
2-4. Pipeline followed for the experimentation . . . . .	16
2-5. Values of Motion added artificially . . . . .	17
2-6. Probabilistic Template of the DMN . . . . .	20
2-7. Baseline: DMN obtained without noise . . . . .	21
2-8. DMN obtained after applying the standard method for motion correction . . . . .	21
2-9. DMN obtained after applying the anisotropic proposed method for motion correction . . . . .	21
2-10.PSNR Results . . . . .	22



# Table list

<b>1-1.</b> Motion in fMRI . . . . .	8
<b>2-1.</b> Experimentation . . . . .	19
<b>2-2.</b> Mean of PSNR for the applied methods . . . . .	23
<b>2-3.</b> Percentage of performance . . . . .	23

# Index

<b>Acknowledgements</b>	<b>v</b>
<b>Abstract</b>	<b>vi</b>
<b>Figure List</b>	<b>vii</b>
<b>Table list</b>	<b>ix</b>
<b>List of Symbols and abbreviations</b>	<b>xii</b>
<b>1. Introduction</b>	<b>1</b>
1.1. Resting State Networks -RSN- . . . . .	1
1.2. Default Mode Network -DMN- . . . . .	2
1.2.1. Functional analysis of regions of the DMN . . . . .	3
1.2.2. Micro-structure of the regions of the DMN . . . . .	5
1.3. Functional Magnetic Resonance Imaging -fMRI- . . . . .	5
1.4. Artifacts in fMRI . . . . .	7
1.5. Document organization . . . . .	10
<b>2. Method for detection of the Default Mode Network using Anisotropic Analysis of Functional Data</b>	<b>11</b>
2.1. Introduction . . . . .	11
2.1.1. Basal Ganglia . . . . .	12
2.1.2. Anisotropy . . . . .	14
2.2. Methodology . . . . .	15
2.2.1. Noise addition . . . . .	16
2.2.2. Preprocessing . . . . .	16
2.2.3. Motion Correction . . . . .	17
2.2.4. Processing . . . . .	18
2.2.5. Datasets and experimental setup . . . . .	20
2.3. Results . . . . .	20
2.3.1. Performance Analysis . . . . .	22
<b>3. Discussion, Conclusions and Future Work</b>	<b>24</b>
3.1. Discussion . . . . .	24

3.2. Conclusion . . . . .	24
3.3. Future Work . . . . .	25
<b>A. Appendix 1: Presented Article</b>	<b>26</b>
<b>Bibliography</b>	<b>35</b>

# Symbols and abbreviations

## Abbreviations

Abbreviation	Meaning
<i>BG</i>	Basal ganglia
<i>CBF</i>	Cerebral Blood Flow
<i>DMN</i>	Default Mode Network
<i>DVARs</i>	Derivative variation
<i>EPI</i>	Echo planar Imaging
<i>FD</i>	Frame wise displacement
<i>fMRI</i>	Functional Magnetic Resonance Imaging
<i>GPe</i>	Globus pallidus external
<i>GPi</i>	Globus pallidus internal
<i>MRI</i>	Magnetic Resonance Imaging
<i>MSE</i>	Mean Square error
<i>PET</i>	Positron Emission tomography
<i>PSRN</i>	Peak signal noise to ratio
<i>rs – fMRI</i>	Resting State Functional Magnetic Resonance Imaging
<i>RSN</i>	Resting State Network
<i>SNc</i>	Substantia nigra pars compacta
<i>SNr</i>	Substantia nigra pars reticulata
<i>STN</i>	Subthalamic nucleus

# 1. Introduction

Recent studies of the brain have become non invasive, and they allow to study not only the structure of the brain but also its functionality through images. Medical Imaging, such as, computerized tomography CT, positron emission tomography PET, electroencephalographs EEC and also functional magnetic resonance imaging fMRI are techniques currently used by researchers to get and analyze data that facilitate the understanding of the brain and pathologies associated with it. However, these techniques present some issues such as noise, artifacts and limitations for the analysis of the data. This document is focused on the technique of resting state functional magnetic resonance imaging (rs-fMRI), and presents a methodology that is bio-inspired in the directional and hierarchical flow of the information through the structures of neural tissue. This methodology is proposed for the restoration of the information of activation of the DMN and detect it in rs-fMRI with artifacts caused by head movement.

The proposed method is inspired by how is the information's flow through brain structures. Specifically under the hypothesis information is hierarchically reconstructed from the bottom to the top, as described for the basal ganglia models [1]. At a micro-structural level, the brain is composed of specialized groups of neurons organized in layers that constitute the ganglia, which are the macroscopic visible structures interacting and setting brain functions and stages. The flow of information through these structures has a preferential direction defined by the hierarchy itself, a condition herein exploited by the use of anisotropic filters that reconstitute a particular functional net, the DMN that is artificially perturbed by motion. The model and the proposed methodology are hereafter explained.

## 1.1. Resting State Networks -RSN-

Cognitive studies tested evoked potentials, also called evoked response, refers to the electro physiologic activity or response of the brain to a variety of sensory stimulus of specific sensory nerve pathways[2]. Studies of evoked potentials were important for the understanding of brain functionality, using an electroencephalograph EEG the signal represent summed activity within a specific area of cortex that creates a current flow. In 1929 the inventor of the EEG, Hans Berger, recorded regular and low frequency cerebral fluctuations using EEG when people was at resting, it indicated that the brain was active even in resting state [3]. However, these measurements were considered as uninformative noise and not worthy of

investigation. Decades after, similar fluctuations were identified at resting by using neuro-imaging techniques and the attention on the importance and utility of these fluctuations at resting state increased. These fluctuations also were present in specific regions on the brain which have specific functions. All this was interpreted as potential biomarkers for understanding pathologies or brain abnormalities.

Resting state functional magnetic resonance imaging (rs-fMRI) consists of the acquisition of fMRI data while the person is resting with closed eyes. Typical resting experiments are of the order of 5-10min. These studies are focused on spontaneous low frequency fluctuations ( $0,01Hz < f < 0,1Hz$ ) in the blood oxygenation level dependent (BOLD) signal. Rs-fMRI allows to identify RSN through the inspection of synchronous activations between regions that are spatially distinct, occurring in the absence of a task or stimulus. The low-frequency fluctuations in BOLD have shown to be temporally correlated within spatially distinct but functionally related RSN.

Researchers apply several methods to analyze resting state data and to identify correlations of activation among the voxels. Consistent regions of the brain have been found active during rest, and also it has been identified that these activations decreased when cognitive tasks were performed. The most common method is independent component analysis ICA, but seed voxel analysis is also widely used. Using these methods, have been reported different RSN, in Figure 1-1 are shown some of the RSN identified during researches.

Several resting state networks RSN have been identified, i.e: default mode network, somato-motor network, visual network, language network, dorsal attention network, ventral attention networks fronto control network, auditory network, cingulo opercular network.[5]. The network that has been widely identified and also the most studied network is the default mode network DMN.

Clinical uses of RSN is at an early stage of developments and are still under study. Especially the DMN has shown promising results to be used in clinical applications such as prognosis, diagnosis and control of neurological and psychiatric diseases [6].

## 1.2. Default Mode Network -DMN-

Rs-fMRI studies have shown evidence of resting state networks (RSN), the most known of these networks is called default mode network (DMN) it refers to a group of interconnected brain structures that are hypothesized to be part of a functional system activated when the person is awake but not involved in any specific mental exercise. There is not yet a complete consensus on which brain regions should be included in a definition of the DMN, but it is usually identified in the posterior cingulate cortex (PCC) and anterior medial prefrontal cor-

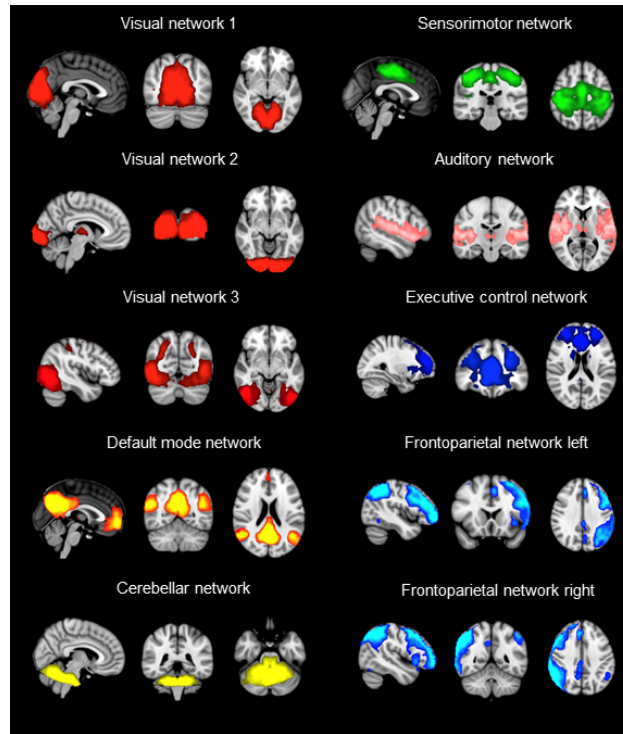


**Figure 1-1.:** Resting State Networks reported by Smith et al, 2009.[4].

tex (mPFC). The DMN also has been associated to other structures that may be considered part of this network, they are the precuneus, the bilateral parietal cortex, anterior cingulate cortex (ACC), hippocampus and thalamus. In FIGURE.1-2 is shown a template of the DMN developed by Wang et al, and used to compare the components when an independent component analysis ICA is performed.

Researchers identified that the DMN remains active during episodic and autobiographical memory retrieval, but its activity decreases during the performance of cognitive tasks that demand attention to external stimuli. Other studies have reported alterations on the DMN activation when the acquisition was done in people in special states; such as deficit of consciousness[8][9], or with pathologies i.e Alzheimer's disease (AD) [10], Migraine, schizophrenia. For this reason the DMN have been proposed and studied as biomarker for those pathologies.

### 1.2.1. Functional analysis of regions of the DMN

The DMN is identified by using different techniques such as PET and rs-fMRI. It is identified as a group of interconnected brain structures. These structures are apparently are part of

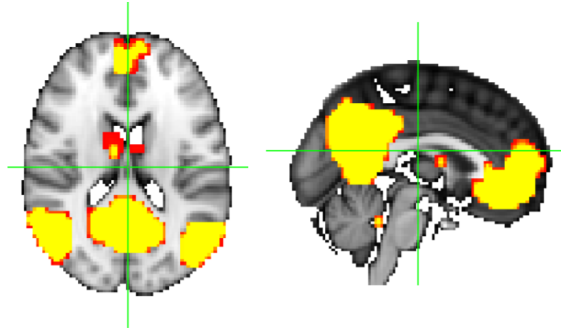


**Figure 1-2.:** Default Mode Network.  
Regions were reported by Bruckner et al, 2008 [7].

a functional system activated when people are not involved in any mental activity. Some of the structures related to the DMN are introduced hereinafter.

- **The posterior cingulate cortex (PCC)** lies behind the anterior cingulate and is active during the recall of autobiographical memories it is also activated by emotional stimuli.
- **The medial prefrontal cortex (mPFC)** is composed of granular cortical areas and agranular regions which encompasses the anterior cingulate cortex infralimbic cortex, and prelimbic cortex.
- **The prefrontal cortex** is highly interconnected with much of the brain, including extensive connections with other cortical, subcortical and brain stem sites. The prefrontal cortex also receives inputs from the brainstem arousal systems, and its function is particularly dependent on its neurochemical environment.
- **The precuneus** is located on the medial surface of the cerebral hemisphere, functionally it is hypothesized to be involved in a variety of functions, ranging from memory to consciousness.
- **The thalamus** has a major role as a gatekeeper for information on its way to the cortex, making sure that the information gets sent to the right place, it relays between sensory and motor systems and the cerebral cortex. It is also involved in consciousness and arousal.
- **The hippocampus** is a structure in the temporal lobe which plays an important role in memory consolidation.

### 1.2.2. Micro-structure of the regions of the DMN

The brain can be seen as a complex structure organized in different brain areas, with different subregions, inside each subregion is divided into layers, and each layer composed by various cell types. At any of the scales of spatial resolution it is possible to identify the response of the neuronal population as a whole.

The hypothesis of columnar organization was first presented by Mountcastle in 1957 [11]. The classical idea of laminar organization of the cortex was dominant and suggested for functional specificity for every cellular layers. Physiological observations generated the hypothesis of the columnar organization required two sets of anatomical facts, these are: 1- neurons in the cerebral cortex are organized horizontally into laminae and 2- they are organized vertically into columns and modules.

The modular organization of nervous system is a widely documented principle of design for brains, the columnar organization of the neocortex is an example. Classical architectural areas of the cortex are composed of small units it is local neural circuits repeated iteratively within each area. Modules may vary according to the cell type and quantity, in internal and external connectivity. Modules are most commonly grouped into entities by sets of dominating external connections columnar defining factors in homo typical areas and they are generated, in part, within the cortex itself. In figure 1-3 a representative column neocortex is presented.

## 1.3. Functional Magnetic Resonance Imaging -fMRI-

MRI is a technique where a magnetic scanner is used to generate a 3D image. Basically, the magnetic field of the magnet is used to align the protons of hydrogen nuclei from the object and by applying a radio frequency pulse on resonance that cause the absorption and emission of energy in the protons. The retransmitted energy is used to form an image after transformations of the values of energy to intensities.

Functional resonance imaging (fMRI) refers to a imaging technique that provides a tool for visualizing neural activity in the human brain in a non invasive way. fMRI allows to identify the brain activity using 4D images (3D space and 1D time). This technique was developed after the observations of cerebral blood flow (CBF) [13], specifically the venous blood oxygenation level dependent (BOLD)[14] and magnetic resonance imaging (MRI). Image formation in this technique is possible because deoxyhemoglobin (dHb) is like an exogenous paramagnetic contrast agent and alterations in the signal intensity of MRI have been identified if there are changes in the local dHb concentration in the brain [10] and by this way is

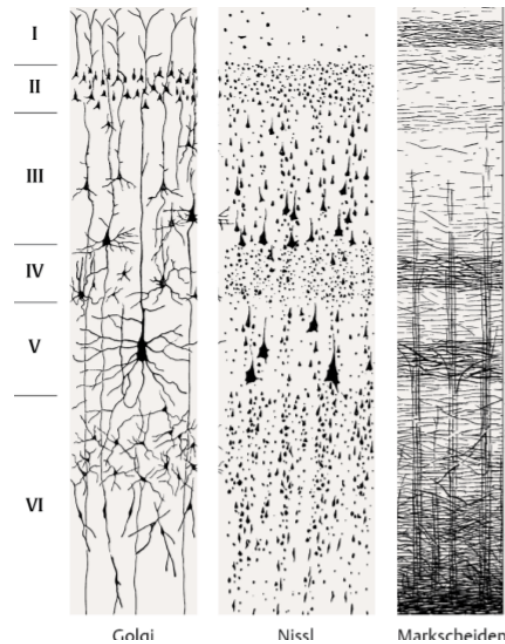


**Figure 1-3.:** Diagram representative of column neocortex.  
Image source: [12].

possible to map brain functions. BOLD does not measure neuronal activity directly, it measures the metabolic demand of active neurons. In other words, BOLD induces changes in the local magnetic susceptibility and these can be measured by Gradient Echo-Planar-Imaging (EPI).

The fundamental unit of a 3D image is called voxel (volume element). Each voxel represents a spatial intensity associated to a location. Taking into account the size of a neuron, a voxel of 1x1x1 mm could represent the activation signal of a population of almost 100.000 neurons. Because of this, the voxel size determines the resolution of the image (the smaller size corresponds to a higher resolution of the image). Voxels in the same plane represent a slice. The 3D image is composed by several slices along an axis, these slices are grouped in order to form a volume.

In fMRI, volumes are captured several times, they and the values of BOLD are projected along time. The temporal resolution is limited by the haemodynamic response to a few seconds. In fMRI, voxels of a volume contain the BOLD signal value at an instant in the time. When a study in fMRI is done, an anatomical volume of MRI is taken using the T1 and T2 signal. Moreover, several volumes of T2\* are taken along time.

This is because while MRI allows high spatial resolution, fMRI allows a good temporal resolution but low spatial resolution. So, the anatomical volume MRI is used to analyze the anatomy and structure of the brain and fMRI is focused on understanding neural activity

through visualization of metabolic process in maps of activation.

A functional map or map of activation is generated from fMRI dataset when the signal intensities of images obtained during control and stimulation periods are compared on a voxel-by-voxel basis [10]. Active voxels are those that pass a statistical threshold based on correlation, they are color-coded based on statistical values (i.e. t-values). Then, the functional map formed by this voxels is overlaid on an anatomical image to enhance the visualization.

Researchers and specialists have used fMRI to investigate and visualize brain functions including memory, vision, motor, language and cognition. For these studies, images acquisition is done during repeated control and stimulation periods. Studies in resting state have been also applied [15], it is known as rs-fMRI, and consists in data acquisitions while the people is resting quietly with their eyes closed.

## 1.4. Artifacts in fMRI

In fMRI have been detected and reported artifacts [16]. The artifacts are basically described as an inaccurate effect or unwanted events observed in a scientific investigation or from experimental error. They are not naturally present but occur during the acquisition of the image and cause signal loss or added noise to the resulting image. There are different types of artifacts in fMRI and they are caused by different sources. For example, artifacts can be result of a malfunction in the hardware or software of the scanner or another device. They can also be a consequence of environmental influences as heat, chemical or humidity. The body of the scanned person can cause artifacts, too. Although there are many kind of artifacts caused by the physiology, and specifically by voluntary movement such as head movement, or involuntary i.e. respiration and cardiac activity. This work has been focused on the treatment of images with artifacts caused by head movement, basically because it posses significant challenges for the analysis of data acquires from children, older adults and patients with dementia[5].

Artifacts caused by head movement correspond to alterations of the signals captured during the acquisition when the person moves his or her head, this is problematic for several reasons: 1) Activation caused by head motion can be correlated with activation due to processing in response to an experimental condition. 2) Head motion increases residuals, resulting in weaker statistical effects. 3) Head motion causes changes intensity of activation at the voxel level. [17]. In clinical fMRI, the major contribution to signal artifacts comes from bulk head motion during the functional data series. Physiological brain motion driven by cardiac pulsations also is a minor contribution. Thus, the main reason for most failed clinical fMRI examinations is motion. For example, the presence of head motion artifacts was the most

**Table 1-1.:** Motion in fMRI.

Adapted from [17]

	<b>Description</b>	<b>Time scale</b>	<b>Effects on the acquired image and the functional map</b>
<b>Intra-image</b>	Fast and sudden motion	Smaller than the image acquisition time scale	Blurring and ghosting. Changing the contrast in the images
<b>Inter-image</b>	slow movement	Between a couple of seconds and minutes.	Leads misregistration of the images within the time series, and makes activation foci undetectable or induces artefactual activation when it is temporally correlated to the stimulus.

frequent cause for the failure in the study of Krings et al [18].

Head motion can be represented as a rigid body movement, that is, person's head motion can be represented with six parameters (three translations and three rotations). However, as was demonstrated by Friston et al.[19]. Motion correction does not restore the signal only by registrations.

FIGURE. 1-4.

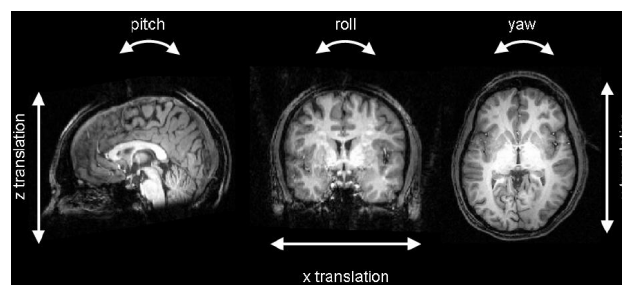
**Figure 1-4.:** Head motion

Image source:[17].

During the acquisition, head movement can be restricted by fixation of the head with molds and straps. A ‘bite-bar’ can also be used to provide a highly rigid fixation but its use is limited to a low number of people and most patients can not tolerate this fixation. To summarize, movement can not be avoided only systematically decreases the signal, especially for larger movements. Motion can also cause variable disruptions, that can be brief or surprisingly long, impacting correlations for up to 10s [20].

Motion tends to increase correlations with predominantly lateral orientations, and decrease those with predominantly vertical or anterior – posterior orientations [16]. Some researchers have focused their works on this problem and they have identified, characterized and developed some methodologies to reduce the effects of artifacts caused by head movement artifact. A posteriori correction of head movement algorithm is an option for solving this issue caused by the head movement during the acquisition.

Nowadays, the motion correction is achieved by rigid realignment of the consecutively acquired images in the data series with the first or middle volume. If the patient moved with a frequency unrelated to the frequency of the applied stimulation paradigm, then this realignment post-processing can successfully separate this motion from true activation.

Most motion correction algorithms are intensity based, and this can facilitate that a false motion could be observed in the time series which is actually the result of a large activation at a specific brain region shifting the center of intensity in a certain direction following the activation paradigm.

Some motion can be corrected at the pre-processing stage, but there are consequences such as loss information from the top and bottom of the image, or motion correction can lead to blurring of the image. A multi scale method was proposed by Baquero et. al. [9]. A wavelet despiking was proposed by [21]. Kelly et al [22], defined a procedure for artifact removal by visual inspection of independent components (IC) in which described those patterns that correspond to artifacts, basically this work describe how noise patterns are observed as check board activations, ring patterns or activation in regions that do not represent any structural or functional relation. Griffanti proposed a method based on Independent component analysis (ICA) to identify and remove sources of signal related to noise [23].

Motion regressors were also studied and proposed as option for solving motion issues [20]. Satterwhite described the spatial, temporal, and spectral characteristics of motion artifact in rs-fMRI data. This study also proposed that motion artifact is relatively spatially distributed, temporally constrained, and frequency-nonspecific.

Although all those researches have improved in some way the detection of the DMN, head motion causes that after the analysis the spatial map of the network does not correspond with the one is known, instead of that the analyst can identify mixed signals and the identification of the DMN is difficult. So, remains an open challenge to identify it in a robust way in order to understand when changes in functional connectivity are or not significantly associated with pathologies.

This study propose an approach based on the hypothesis that information on the brain flows

according to the direction, specifically taking into account the connectivity model of the basal ganglia in which signal travel according to the layer of cells in each nuclei. Mainly this thesis sought to contribute to the goal of enhancing the detection of the default mode network in resting state functional resonance imaging. In order to contribute on this field, the research was focused on the problem of motion correction caused by head motion. Specifically, this thesis presents a methodology centered in the hypothesis of the anisotropy in the information of the images and in the brain and how the use of filters to detect in a better way the default mode network even with high motion added to the images.

## **1.5. Document organization**

This document is organized as follows: In chapter 1 it is introduced the functional resonance imaging, the default mode network and the artifacts caused by head motion, as well as definition of the problem and the necessity of enhancing the detection of the DMN. In chapter 2 is introduced the idea of how the connectivity model of the basal ganglia can be understood as a framework for the use of an anisotropic approach for DMN detection. A generic formulation of anisotropic filters is introduced, with further focus on the use of it in the proposed methodology. Qualitative and Numerical results of the detection of the DMN in rs-fMRI with head motion noise artificially added. Those results are discussed in chapter 3 followed by conclusions and future work.

This document has been structured around the main product of this thesis: a paper submitted to SIPAIM 2017, the 13th International Symposium on Medical Information Processing and Analysis . The paper presents the results of applying the anisotropic proposed approach in order to test the performance of the restoration of the DMN even after motion artificially added. Results show that the DMN detected by using the anisotropic approach has a good performance.

## 2. Method for detection of the Default Mode Network using Anisotropic Analysis of Functional Data

### 2.1. Introduction

Resting state magnetic resonance imaging rs-fMRI is a powerful and non invasive technique in medical imagenology that recently has become in a widely used technique for the detection of resting state networks (RSN) and analysis related with its connectivity. Default mode network (DMN) is one of the RSN that has been widely known and studied, alterations on its connectivity have been related to the presence of alterations in the brain.

Usually, detection of networks in resting state is difficult because there are artifacts present in the data. Different sources of artifacts can be detected in the images, one of the most common are those caused by head movement. Researches have shown that participant motion is a potential source of error in studies of brain morphometry in clinical and nonclinical populations [24] and also that the stronger the head motion, the fewer networks are detected by data-driven methods such as independent component analysis (ICA).

Researches have detected that functional connectivity measurements also may be significantly influenced by head motion that occurs during image acquisition. [25].

There are methods proposed for remove or decrease that kind of artifacts, as well as measurements that pursuit to characterize those artifacts and establish a better compression of the ways to avoid the effects of them.

The aim of this study was to propose a method for motion correction based on anisotropic filtering of the functional data and compare the results of methods for motion correction and its utility for the detection of the DMN. Data from the performance of various methods for motion correction (a standard method and the proposed one using anisotropic filter) are compare and results of the transformations performed are presented.

### 2.1.1. Basal Ganglia

The human brain is composed of a number of different regions. These regions control specific functions. It is usual to identify in the brain the gray matter, the white matter and the cerebrospinal fluid (CSF). The brain is symmetric in composition, but not in size nor volume. The basal ganglia (BG) is a set of subcortical nuclei composed by gray matter and located in the midbrain, around the thalamus. The structures identified as part of the basal ganglia in the brain are: the striatum, the globus pallidus the subthalamic nucleus (STN) and the substantia nigra. Although some authors highlight the fact STN and substantia nigra are not part of the basal ganglia, they recognize the importance of those nuclei for the connectivity and function of the BG. The striatum comprises the caudate nucleus, putamen, ventral striatum and even the nucleus accumbens. The globus pallidus is basically composed by an external segment (GPe) and an internal segment (GPi) easily differentiable especially at the histological level as can be seen in **2-2** . The substantia nigra usually is divided into the pars reticulata (SNr) and the pars compacta (SNc)[1].

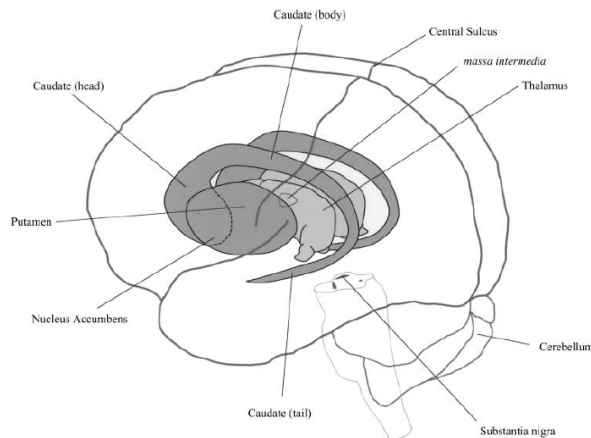


**Figure 2-1.:** Basal Ganglia.

Image source: [26] It presents the main parts that compose the basal ganglia.

The nuclei of the BG have subdivisions that indicate functional organization [1]. The functionality of the BG is in essentially the control of cortical activity. The BG acts like a brake to prevent unwanted movement. This is done in the cortico-basal loop which basically allows flow of information between the basal ganglia and the cerebral cortex and the frontal lobe via the thalamus. As was observed by Deana Greene [28] the basal ganglia is structured by layers of cells to the striatum, specifically medium spiny neurons (they have large dendritic trees that can form from multiple cortical neurons as well as feedback from the thalamus).

In order to understand this loop and functionality, several models have been proposed. For Nambu [29] the basal ganglia can be seen as four parts with specific tasks: input, output, connecting and modulatory. Striatum and STN allow the input tasks receiving cortical inputs. GPi and SNr project outside the BG to the thalamus and the brain stem. The GPe



facilitation of movements. Direct pathway provides positive feedback to the motor cortices. Indirect pathway inhibits cortical motor neurones this causes inhibition of spinal motor neurones and inhibition of movement. Indirect pathway provides negative feedback to the motor cortices. The two pathways work together to modulate the output of the GPi this output to the thalamus is inhibitory in nature. The thalamus controls the level of excitatory stimulation of the premotor cortex through the amount of inhibition. The BG contributes to the initiation of movement by arousing executive motor centres via a disinhibitory mechanism [31].

Taking the previous explanation of the pathways in BG and just as an introduction to the anisotropic filters and the edge stopping functions, it is important to mention the manner in which the information flows in the BG thanks to the layers it is formed and the way the pathways work in parallel for motion inhibition or excitation which is the basic ideas of inspiration for the methodology proposed in this document.

## 2.1.2. Anisotropy

### Anisotropic Diffusion

A diffusion process is a physic process that try to minimize differences in a spatial concentration of a substance  $u(x, t)$ . This process is described by two equations Fick's Law and continuity equation.

Just to know and to explore thos foundation, by one hand, the Fick's equation enunciate that  $j = -g\nabla u$  where  $\nabla u$  is the gradient concentration, basically it describes the difference  $u_{i-1} - u_i$  and  $j$  represents the substance flow. Finally,  $g$  is the diffusivity, it describes the speed of the diffusion process. Diffusivity depends on the substance and can it can be represented as scalar or a matrix.

By the other hand, the continuity equation represents how the change in time depends on the flow's divergence  $\delta_t u = -div j$  divergence is the spatial derivative of the flow, it means the change that occurs going in or going out, in terms of intensity for images it means how much it increases or decreases. Divergency of  $j \equiv \nabla \equiv \delta_x j_1 + \delta_y j_2$

Finally, the diffusion equation can be obtained replacing the terms of equation 1 in equation 2.  $\delta_y u = div(g\nabla u)$  this equation represents the derivative on the time of the concentration that is equal to the divergence of the times that the gradient is diffused. can be smoothed with Gaussian kernels of increasing width  $\sigma$ . A diffusion process has the form

$$\begin{cases} \delta_t u(x, t) = \Delta u & \text{Differential equation} \\ u(x, 0) = f(x) \forall x \in \Omega & \text{initial condition of the boundary} \\ \delta_n u |_{\delta\Omega} = \langle \nabla u, n \rangle |_{\delta} = 0n & \text{Norm of the derivative} \end{cases}$$

The function  $g$  describes the diffusion.

The idea of using anisotropic diffusion for image processing became stronger with Perona and Malik's work, they presented the first formal description of anisotropy. Exactly, they established three criteria for generating multi scale semantically meaningful: Causality, Immediate Localization and Piecewise Smoothing. They also demonstrated that the simplest version of anisotropic diffusion can be applied with success to multi scale image segmentation[32]. And they proposed a function for edge stopping based on this concept of anisotropy. The anisotropic diffusion equation is:

$$I_t = \text{div}(c(x, y, t))\nabla I = c(x, y, t)\Delta I + \nabla c + \nabla I$$

where  $\text{div}$  indicates the divergence operator, and with  $\Delta$  and  $\nabla$  respectively represent the gradient and Laplacian operators, with respect to the space variables. It reduces to the isotropic heat diffusion equation  $I_t = c\nabla$  if  $c(x, y, t)$  is a constant.

After that, other researches have done contributions to the formulations and the comprehension of the anisotropic diffusion method.

Weickert has contributed widely to this topic, through his analysis and comprehension of the anisotropic diffusion in image processing foundations [33]. He also introduced an explicit discretization for coherence-enhancing anisotropic diffusion filtering which uses first-order derivative approximations that have been optimized for rotational invariance [34]. This work was previously optimized with an algorithm based on 5x5 stencils allowing a better behavior for rotational invariance and avoiding blurring artifacts [35].

Gerig et al, proposed a post process based on anisotropic diffusion. Extensions of a new technique support 3D and multi echo MRI, incorporating higher spatial and spectral dimensions. They demonstrated efficient noise reduction and sharpening of object boundaries.[36]

Ding presented a particularly useful technique for smoothing diffusion tensor images in which direction information contained in the tensor needs to be restored following noise corruption and preserved around tissue boundaries.[37]

Researches as the one done by Zuo [38] suggested that Non Local Diffusion-based spatial smoothing maybe more effective and reliable at improving the quality of both MRI data preprocessing and default network mapping, and have proposed anisotropic diffusion and non-local diffusion kernels.

## 2.2. Methodology

An overview of the pipeline followed for the experimentation is presented in Figure. 2-4. This pipeline starts by the introduction of artificial noise, then the usual pre-processing applied to both functional and anatomical data. Then a motion correction method. Afterwards, an

independent component analysis ICA is carried out followed by the usual DMN template detection.

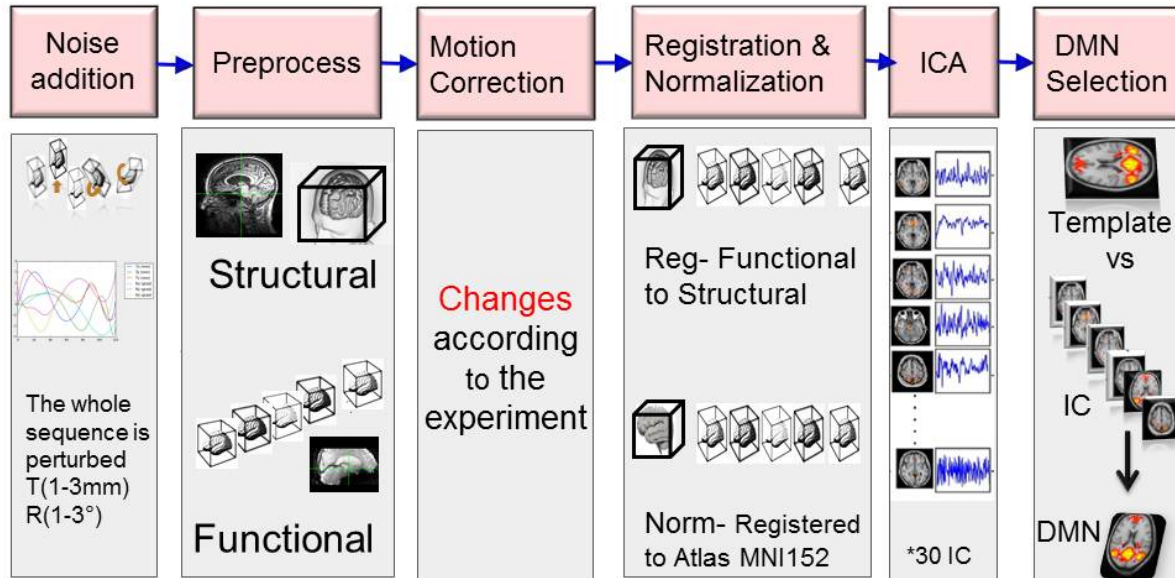


Figure 2-4.: Pipeline followed for the experimentation

### 2.2.1. Noise addition

In order to validate the method, images were altered with artificial noise. For this, volume from each fMRI dataset were transformed spatially in order to simulate head movement, this process was done applying an affine transformation matrix with randomly values for displacement between -3 and 3 mm and with values between -3 and 3 degrees for rotation in in all the axes. Figure.2-5 shows the values of motion applied by following the method for noise simulation in fMRI presented by Ivanna Drobnjak in [39].

### 2.2.2. Preprocessing

The common preprocessing steps for perform an standard analysis of rs-fMRI consist in reorientation, motion correction, remove non-brain tissues, smoothing spatially and filtering temporally.

Remotion of non brain tissues was done wit brain extraction tool BET [40]. Structural data were spatially smoothed with a 5mm FWHM Gaussian Kernel and functional data were temporally filtered with a high-pass filter using  $0,01Hz$  as cut-off frequency to remove slow drifts. Those parameters were chosen according with [41] [42].

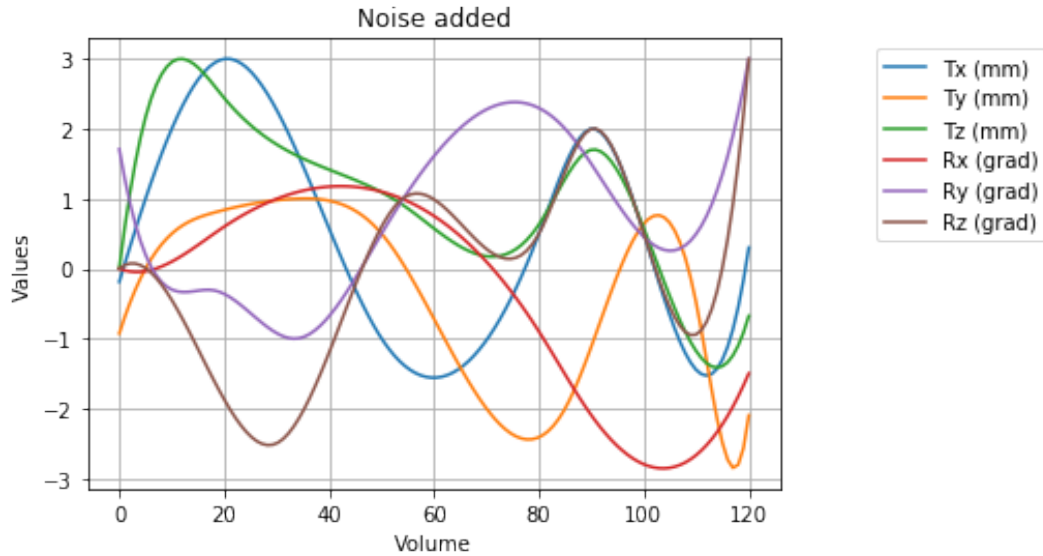


**Figure 2-5.:** Values of Motion added artificially

The registration consists on applying transformations to the functional set of volume to fit it into the anatomical image, a rigid body transformation (6 DoF) was applied, the cost function was correlation ratio and the interpolation method was trilinear. The normalization refers to transformations required to fit the image to the standard space [43] MNI152  $2x2x2mm$ , the method used for normalizations was volume based registration, it means affine transformations (12 DoF) the cost function and interpolation methods were set in the same way to the registration.

### 2.2.3. Motion Correction

The method for motion correction is usually done by using the tool MCFLIRT developed by Jenkinson[44]. This method basically consist in an optimized process of linear registration. This method was used as the method to compare our results.

#### **Approach: A bio-inspired model of the Basal Ganglia**

We hypothesized that flow of information depends on the direction and near points in space existence of significant structural and functional connections between the thalamus and the precuneus and between these regions and other areas in the DMN. For this reason the approach include an anisotropic methodology that is compared with a standard process for the detection of the DMN in dataset altered with artificial artifacts. Evidence suggests information may travel through preferential direction in basal ganglia. This amounts to think information propagates anisotropically. It is also very likely information in other brain regions, is anisotropically propagated. These regions present a layered histological structure.

## Anisotropic filtering

We hypothesize that the flow of information depends on the anatomic direction, modified by the functional connections between the thalamus and the precuneus and between these regions and other DMN areas. Yet neurons are on the order of micrometers, they are structurally connected into layers which have been widely described in many histology treaties. This type of organization allow us to infer that the flow of information at the level of voxels is also anisotropic. This hypothesis is at the very base of the present investigation and is introduced by an anisotropic filter into the usual workflow analysis. The anisotropic filtering herein used aims then to capture the essential information in the dataset altered by artificial motion perturbations. A new implementation of the classic anisotropic filter is out of the scope of the present work. In consequence the filter herein applied was already described by Weickert in [35] and is briefly hereafter described: this filter smooths images by applying the partial differential equation:

$$\frac{\partial I}{\partial t} = \nabla(T \cdot \nabla I)$$

where  $I$  refers to the image intensity,  $\nabla I$  is the intensity gradient,  $t$  is the iteration time parameter and  $T$  is the diffusion tensor. The intensity gradient tensor  $G$  is used to obtain the diffusion tensor  $T$  and is computed by convolving the outer product of the intensity gradient  $\nabla I$  and a Gaussian kernel  $K_\rho$ . It is possible to capture the boundary information that is missing in one direction from another direction by summing  $\nabla I_i \otimes \nabla I_i$  over all directions, followed by a component wise convolution with Gaussian kernel as  $G = K_\rho * \sum(\nabla I \otimes \nabla I)$  and  $\rho$  is the standard deviation of the gaussian kernel and represents the integration scale of convolution. The principal directions and magnitudes of the image intensity gradient  $G$  over the integration scale  $\rho$  are the eigenvectors and eigenvalues of  $G$  respectively. The direction of the largest intensity gradient is the eigenvector associated with the largest eigenvalue and the other way around. The constructed  $T$  smooths then out along the tangential direction of edges. This tensor gives a direction where the diffusion is preferred and another direction where the diffusion is suppressed [37].

### 2.2.4. Processing

#### Structural Information: Registration and Normalization

Each fMRI volume was registered to the subjects high resolution T1-weighted scan using rigid-body registration (6DoF) referring to 3 rotations and 3 translations, for this registration was used the tool FLIRT [45] from FSL. After that, each volume was normalized using volume based approach, it is registering to standard space (MNI152 2x2x2mm) by using affine registration (12DoF).

**Table 2-1.:** Experimentation

<b>Exp</b>	<b>Noise Addition</b>	<b>Pre-processing</b>	<b>Motion correction</b>	<b>Reg and Norm</b>	<b>ICA</b>	<b>DMN Selection</b>
Baseline	No	Yes	<b>No</b>	Yes	Yes	Yes
Compared	Yes	Yes	<b>Mcfirt</b>	Yes	Yes	Yes
Proposed	Yes	Yes	<b>Anisotropic</b>	Yes	Yes	Yes

### **Independent Component Analysis (ICA)**

Once done preprocessing steps, the datasets of all the methods previously mentioned the data was decomposed into 30 independent components (IC) as was used in [9] [46] using Multivariate Exploratory Linear Optimized Decomposition into Independent Components (MELODIC) [47] using simple temporal concatenation. For ICA, the usual supposition is that fMRI data is composed by a mixture of unknown source components which are temporal or spatial independent and uncorrelated and all the IC are non-Gaussian variables. The main criterion of ICA includes minimization of the mutual information, maximum likelihood estimation and non-Gaussian measure. In the parameters a threshold of 0.5 was chosen. And for the IC visualization the BRICON values were establish between 2 and 10.

### **DMN selection**

Although exist criteria for the visual inspection of IC, standardization of denoising and RSN identification [22]. Manual selection of the DMN may be time consuming and a hard work task because all components should be carefully visualized and analyzed. Technical advances have shown the possibility to automate denoising and the identification of the RSN, saving man-hours of highly qualified technical personnel. Here we tested methods for the selection of the DMN based on a measurements of similarity proposed by [48] in order to identify the IC that fit better to the probabilistic DMN template.

### **Probabilistic Template**

All components were compared with a probabilistic template of the default mode network [48], in order to select the more similar component of the DMN. In figure **2-6**

### **Method to Select the DMN**

In order to get the IC most similar to the DMN, the IC obtained from ICA were compared to the template using a similarity measurement proposed by Wang et al, [48].

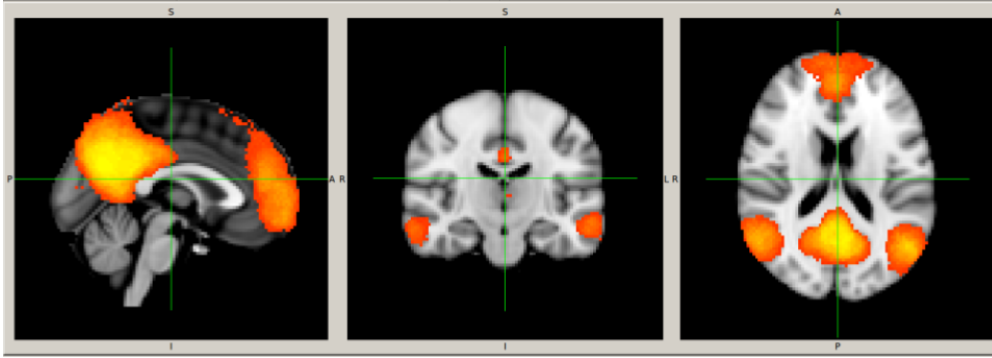


**Figure 2-6.:** Probabilistic Template of the DMN developed by Wang et al, 2014 [48]

$$S = \left| \frac{1}{M} \sum_{m=1}^M \left[ \left( \frac{I_{IC}(m) - \bar{z}_{IC}}{\sigma_{IC}} \right) \left( \frac{I_T(m) - \bar{z}_T}{\sigma_T} \right) \right] \right|$$

where  $S$  is a score obtained to compare the similarity among the IC, the highest represents a better fitness from the IC to the template, the component with the highest  $S$  is chosen as the DMN.  $z_{IC}$  and  $z_T$  are the values of  $M$  voxels in the common mask of the IC and the template, respectively.  $\bar{z}_{IC}$  and  $\bar{z}_T$  are the mean values of  $z_{IC}$  and  $z_T$ , respectively, and  $\sigma_{IC}$  and  $\sigma_T$  are the corresponding standard deviations.

### 2.2.5. Datasets and experimental setup

Rs-fMRI from 14 healthy people were used (Mean age: 75,5 years. Women: 12). For all subjects, data were acquired with the following features: TR:2500 ms, TE: 27,5 ms, Echo spacing: 772 us, Asset: 0,5, volume: 120, Slices: 32 and Voxel dimension: 2,5x2,5x2,6 mm.

## 2.3. Results

The qualitative results are shown in figure 2-7,2-8 and 2-9 DMN obtained after the experimentation with data from a subject. The column 2-7 shows the DMN obtained as baseline. It is without noise and without applying any motion correction method. The figure 2-8 belong to the views of the DMN obtained after introducing artificial head movement and also applying the state of art method for motion correction (Mcflirt)[44]. The third figure 2-9 belong to the DMN obtained after introduce artificial noise and applying the anisotropic approach for motion correction. A better detection of DMN is observed after applying the anisotropic method.

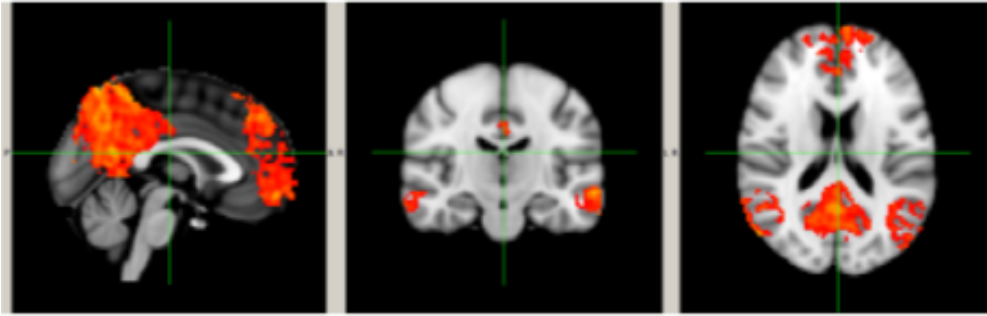


**Figure 2-7.:** Baseline: DMN obtained without noise

This DMN belong to the first subject, for the detection artificial noise was not added and any method for motion correction was used.

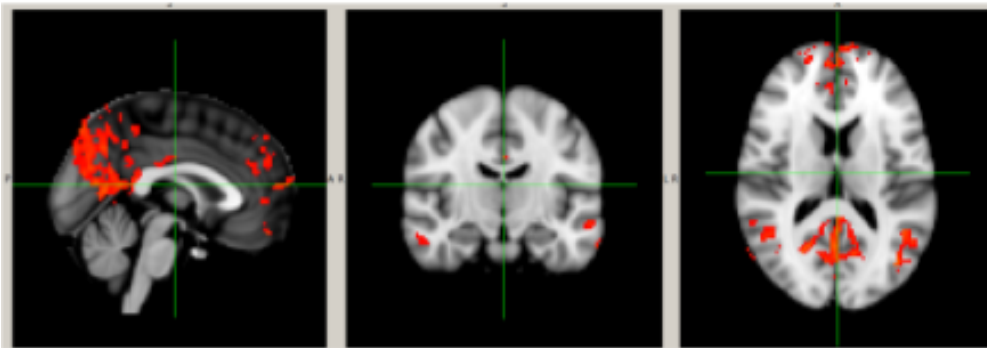


**Figure 2-8.:** DMN obtained after applying the standard method for motion correction

This DMN belong to the first subject, data were corrupted with artificial noise to simulate head motion and the method used for motion correction is a optimized registration.

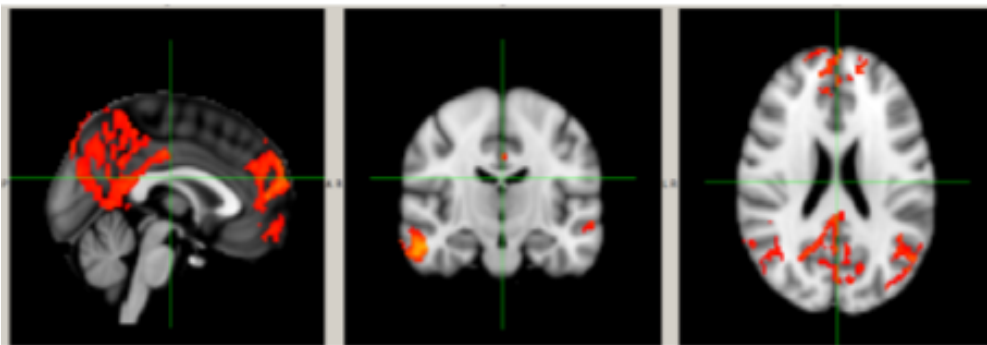


**Figure 2-9.:** DMN obtained after applying the anisotropic proposed method for motion correction

This DMN belong to the first subject, data were corrupted with artificial noise to simulate head motion and the method used for motion correction is an diffusion anisotropic filter.

### 2.3.1. Performance Analysis

In order to test and validate the method, the baseline image  $I_{ref}$ , corresponding to the DMN obtained with the without noise and neither motion correction process, was compare to the image  $I_{test}$  which correspond to the DMN obtained after applying noise to the image and using one of the two methods for motion correction (the proposed one or the standard). Measurements of peak signal noise ratio PSNR.

#### PSNR

PSNR was computed by taking the mean squared error (MSE) between the voxel intensities of the Baseline DMN and the DMN obtained after applying the method with the anisotropic filter. This is an objective measure for test the quality of a reconstructed image, the one altered with noise, with respect to the baseline image.

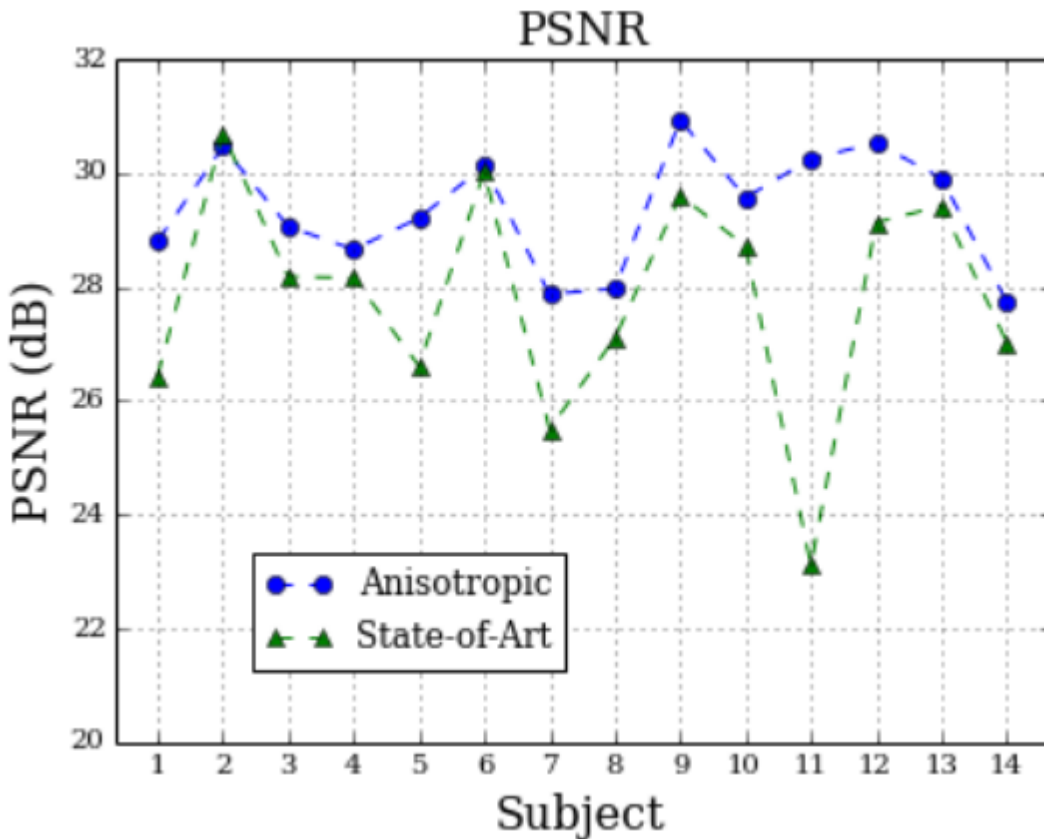


Figure 2-10.: PSNR Results

In this graphic the results of PSNR are presented. The values of the DMN acquired using the anisotropic approach outperform the PSNR values of the DMN acquired with the state-of-art method

**Table 2-2.:** Mean of PSNR for the applied methods

	Mean Anisotropic	Mean state of art
PSNR	29.35	27.83

**Table 2-3.:** Percentage of performance

Measurement	Percentage
PSNR	5.93

# 3. Discussion, Conclusions and Future Work

## 3.1. Discussion

A voxel is nothing but the space location of the average activity of a large population of neurons. The way the nervous systems processes information is essentially hierarchical, that is to say from the environment, where information is more or less linearly represented by captors, to the central networks, dimensionality is reduced aiming to extract the most relevant information. This hierarchical construction of the external world is by nature anisotropic, that is to say information is wired from many to few. Anatomical and histological evidence supports this claim, neurons communicate with networks that highlight the essential part of the information and this is performed by specialized architectures, columns or layers, whose main role is to select relevant information.

A method for enhance the detection of the DMN was proposed inspired on the organization of neural cells in the basal ganglia. The method was tested and compared the results with a metric of PSNR.

The contribution presented is a method inspired in the model of how information is propagated and the use of this to improve the DMN restoration when some motion perturbs the network. This method for enhancing the detection of the DMN was proposed inspired on the organization of neural cells in the basal ganglia. This method was tested and compared the results with a metric of PSNR.

## 3.2. Conclusion

The study proposes an anisotropic analysis of the information flow in rs-fMRI to correct artifacts caused by head motion. The results show an improvement in the DMN detection, less variability in the response of the DMN and a better detection by applying the anisotropic method. Results obtained show that the anisotropic approach outperforms the state-of-the-art method by 5.93 % PSNR.

The contribution presented is a model of how information is propagated and the use of this

to improve the DMN restoration when some motion perturbs the network. This analysis is inspired by the fact that the nervous systems reduces dimensionality by structuring information hierarchically and anisotropically. This simple modification results to be very efficient in terms of recovery of the network perturbed by artifacts caused by head movement.

### 3.3. Future Work

The proposed method shows a better detection of the DMN even with altered images. Experimentation with a large dataset could be reinforce the validity of results through a statistical test. Variability among the population also can be tested, it means the use of the the anisotropic approach in images from people whit pathologies or states that induce head motion during the acquisition taking into account the motion patterns characteristic of the pathology or state analyzed. This work was focused on artifacts caused by head motion in rs-fMRI, however the analysis combining information from images acquired with different techniques (i.e PET or DWI) also could be possible.

An interesting way to continue exploring and modeling the information's flow for the detection of resting state networks in rs-fMRI altered by head movement is the work with fluid equations. This approach could model in a best way the information's flow following rules of dynamic of fluids, using techniques such as finite elements, finite differences and finite volume.

Another way could be the use of machine learning techniques such as convolutional neural networks that employ intelligent filters. Here, a neural network can be trained to adapt itself to the dynamic of historic images. For both, analysis and quantification of functional connectivity performance could be required.

## **A. Appendix 1: Presented Article**

The following article was presented at 13th International Symposium on Medical Information Processing and Analysis SIPAIM 2017. Conference proceedings are expected to be published by SPIE Digital Library.

# Detection of the Default Mode Network by an anisotropic analysis

Aura Forero and Eduardo Romero<sup>a</sup>

<sup>a</sup>Computer Imaging and Medical Applications Laboratory(CIM@LAB), Universidad Nacional de Colombia , Bogotá, Colombia

## ABSTRACT

—This document presents a proposal devoted to improve the detection of the default mode network (DMN) in resting state functional magnetic resonance imaging in noisy conditions caused by head movement. The proposed approach is inspired by the hierarchical treatment of information, in particular at the level of the brain basal ganglia. Essentially, the fact that information must be selected and reduced suggests propagation of information in the Central Nervous System (CNS) is anisotropic. Under this hypothesis, the reconstruction of information of activation should follow an anisotropic pattern. In this work, an anisotropic filter is used to recover the DMN that is perturbed by simulated motion artifacts. Results obtained show this approach outperforms the state-of-the-art methods by 5.93% PSNR.

**Keywords:** Anisotropic diffusion filter, Motion correction, head motion, default mode network, rs-fMRI

## 1. INTRODUCTION

Recent studies of the brain include the acquisition of anatomical and functional images. Computerized tomography CT, positron emission tomography PET, electroencephalographs EEC and magnetic resonance imaging MRI are techniques for acquiring brain images. These images are analyzed with different methods. Results of these analysis facilitate the understanding of the brain and pathologies associated.

This document is focused in the analysis of a non invasive technique called resting state fMRI. For this technique, a set of images are acquired along time while the subject is not performing cognitive task and with closed eyes. The base of these images is the blood level oxygen dependent BOLD signal. This signal is associated to the magnetic properties of the blood and the metabolism of neural cells.<sup>1</sup> Low-frequency fluctuations in BOLD  $0.01Hz < f < 0,1Hz$ <sup>2</sup> allow to identify resting state networks RSN through the inspection of synchronous activations.

The default mode network (DMN) is the most studied RSN. It has been identified and associated to brain areas such as the bilateral parietal cortex, the precuneus, posterior cingulate cortex (PCC), anterior cingulate cortex (ACC), medial prefrontal cortex (MPFC), hippocampus and thalamus.<sup>3</sup>

Usually, detection of RSN is difficult because there are artifacts present in the data. Different sources of artifacts can be detected in the images, one of the most common is caused by head movement during the acquisition. Researchers have shown that subject's motion is a potential source of error in studies of brain morphometry in clinical and nonclinical populations.<sup>4</sup> Functional connectivity measurements also may be significantly influenced by head motion that occurs during image acquisition.<sup>5</sup> For this reason, many papers have been published specifically concerning the motion artifact issues in resting state fMRI.<sup>6</sup> There are methods proposed for remove or decrease the effects of these artifacts, as well as measurements that pursuit to characterize them.<sup>2</sup> Lineal registration of volumes is one of the methods applied for deal with these issues.<sup>7</sup>

The proposed method is inspired by how is the information's flow through brain structures. Specifically under the hypothesis information flows hierarchically and anisotropically,<sup>8</sup> as modeled for the basal ganglia.<sup>9</sup> At a micro-structural level, the brain is composed of specialized groups of neurons organized in layers that constitute the ganglia, which are the macroscopic visible structures interacting and setting brain functions and stages. The flow of information through these structures has a preferential direction defined by the hierarchy itself, a condition herein exploited by the use of anisotropic filters that reconstitute a particular functional net, the DMN that is artificially perturbed by motion. The model and the proposed methodology are hereafter explained.

The contribution presented in this document is a method inspired in the model of how information is propagated and the use of this to improve the DMN restoration when some motion perturbs the network. This method for enhancing the detection of the DMN was proposed inspired on the organization of neural cells in the basal ganglia. The results of applying this method were tested using metrics of SNR, PSNR and BOLD variation. These results are also compared with results of applying a state-of-art method.

## 2. METHODS

The whole pipeline, is illustrated in Figure 1. This pipeline starts by the introduction of artificial noise, then the usual pre-processing applied to both functional and anatomical data. Then a motion correction method consists in anisotropically filtering out the previously preprocessed data. Afterwards, an independent component analysis ICA is carried out followed by the usual DMN template detection.

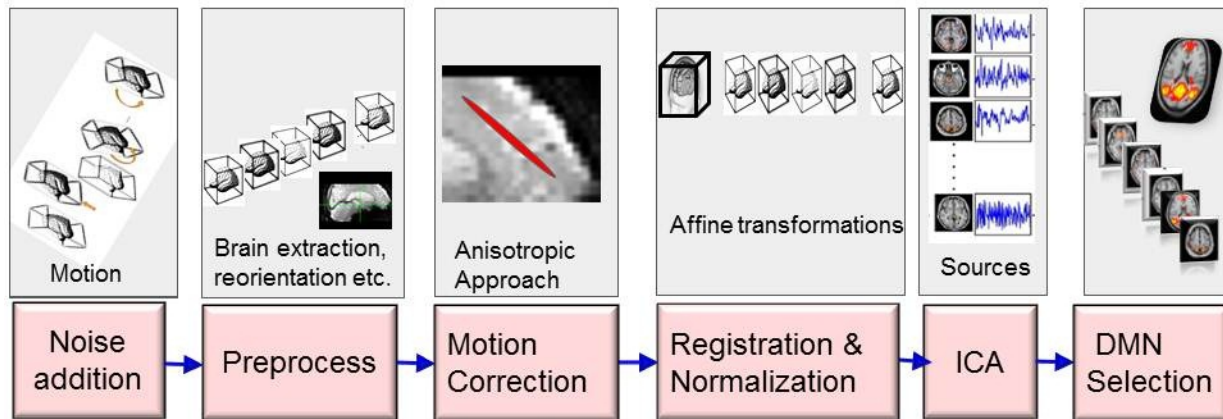


Figure 1: Modified pipeline by introducing the anisotropic filtering

### 2.1 Noise addition

Motion was herein simulated by artificially perturbing the whole sequence. Functional volumes from each rs-fMRI acquisition were spatially transformed to emulate the head movement, as described in<sup>10</sup> where was proposed an approach to simulate the full effects of various rigid-body motion artifacts in FMRI data in a controlled and precise way. The applied affine transformation consisted in displacement values between  $-3$  and  $3$  mm and rotation values set between  $-3$  and  $3^\circ$  of the respective  $x, y$  and  $z$  axes.

### 2.2 Preprocessing

The common rs-fMRI preprocessing steps are reorientation, motion correction, non-brain tissue removing, spatial smoothing and temporal filtering.

Non brain tissues from anatomical volume were firstly removed using the brain extraction tool BET.<sup>11</sup> Structural data were also spatially smoothed with a  $5$  mm FWHM Gaussian Kernel. Functional data were temporally filtered with a high-pass filter using  $0.01$  Hz as cut-off frequency to remove slow drifts as described in<sup>12,13</sup>

### 2.3 Motion Correction

The common pipeline without motion neither correction of motion was herein used as a baseline. Motion is usually corrected by the MCFLIRT tool<sup>7</sup> which implements a linear registration optimized process. DMN obtained by using MCFLIRT was used to compare our results.

### 2.3.1 The Anisotropic Approach

We hypothesize that the flow of information depends on the anatomic direction, modified by the functional connections between the thalamus and the precuneus and between these regions and other DMN areas. Yet neurons are on the order of micrometers, they are structurally connected into layers which have been widely described in many histology treaties. This type of organization allow us to infer that the flow of information at the level of voxels is also anisotropic. This hypothesis is at the very base of the present investigation and is introduced by an anisotropic filter into the usual workflow analysis. The anisotropic filtering herein used aims then to capture the essential information in the dataset altered by artificial motion perturbations. A new implementation of the classic anisotropic filter is out of the scope of the present work. In consequence the filter herein applied was already described by Weickert in<sup>14</sup> and is briefly hereafter described: this filter smooths images by applying the partial differential equation:

$$\frac{\partial I}{\partial t} = \nabla(T \cdot \nabla I) \quad (1)$$

where  $I$  refers to the image intensity,  $\nabla I$  is the intensity gradient,  $t$  is the iteration time parameter and  $T$  is the diffusion tensor. The intensity gradient tensor  $G$  is used to obtain the diffusion tensor  $T$  and is computed by convolving the outer product of the intensity gradient  $\nabla I$  and a Gaussian kernel  $K_\rho$ . It is possible to capture the boundary information that is missing in one direction from another direction by summing  $\nabla I_i \otimes \nabla I_i$  over all directions, followed by a component wise convolution with Gaussian kernel as  $G = K_\rho * \sum (\nabla I \otimes \nabla I)$  and  $\rho$  is the standard deviation of the gaussian kernel and represents the integration scale of convolution. The principal directions and magnitudes of the image intensity gradient  $G$  over the integration scale  $\rho$  are the eigenvectors and eigenvalues of  $G$  respectively. The direction of the largest intensity gradient is the eigenvector associated with the largest eigenvalue and the other way around. The constructed  $T$  smooths then out along the tangential direction of edges. This tensor gives a direction where the diffusion is preferred and another direction where the diffusion is suppressed.<sup>15</sup>

### 2.4 Registration and Normalization

Registration aims to match the set of functional data and the anatomical image (T1-weighted scan), applying rigid body transformations with 6 degrees of freedom (DoF). Afterward, normalization consists in registering these data to the standard  $MNI1522x2x2$  space (Stereotaxic Registration Model),<sup>16</sup> applying affine transformations with 12 DoF. Both, registration and normalization, use the same FLIRT tool<sup>17</sup> from the FS.

### 2.5 Independent Component Analysis (ICA)

After these preprocessing steps, an independent component analysis ICA is applied to data per subject. ICA supposes fMRI data is composed of a mixture of unknown non-Gaussian source components which are temporally or spatially independent. Separation of these non Gaussian sources is achieved by minimization of the mutual information and maximum likelihood estimation. Data are decomposed into sources, the independent components (IC), herein 30 as described in<sup>18,19</sup>.

### 2.6 DMN selection

Several methods for visually classifying the independent components have been proposed.<sup>20</sup> Here, the detection of the DMN is based on the comparison of scores obtained from a similarity metric proposed by Wang et al.,<sup>21</sup> Basically, Wang applied an algorithm for selecting the most similar independent component to a DMN probabilistic template. For this, the z-values of both signals are convolved as shown in Equation (2) to compute the score.

$$S = \left| \frac{1}{M} \sum_{m=1}^M \left[ \left( \frac{I_{IC}(m) - \bar{z}_{IC}}{\sigma_{IC}} \right) \left( \frac{I_T(m) - \bar{z}_T}{\sigma_T} \right) \right] \right| \quad (2)$$

Being  $S$  the score obtained by comparing the similarity between the image of each independent component  $I_{IC}$  and a probabilistic DMN template  $I_T$ . The highest score component represents the highest match to

the DMN,  $z_{IC}$  and  $z_T$  are the  $z$  values of  $M$  voxels in the common mask of the IC and the template, while  $\bar{z}_{IC}$  and  $\bar{z}_T$  are the  $z_{IC}$  and  $z_T$  mean values, respectively, and  $\sigma_{IC}$  and  $\sigma_T$  are their corresponding standard deviations.

### 3. DATASET AND EXPERIMENTAL SETUP

#### 3.1 Dataset

The proposed strategy was assessed in rs-fMRI data from 14 healthy people (Mean age: 75.5 years. Women: 12). For all subjects, data were acquired under the following parameters: TR:2500 ms, TE: 27.5 ms, Echo spacing: 772 us, Asset: 0.5, volume: 120, Slices: 32 and Voxel dimension:  $2.5 \times 2.5 \times 2.6$  mm.

#### 3.2 Experimentation

The dataset described above was used following the steps mentioned in the pipeline proposed to obtain three sets of DMN.

The first group correspond to the baseline DMN, this was obtained skipping the step of noise addition and also the step of motion correction. It is applying the steps of preprocessing, registration, normalization, independent component analysis and DMN selection.

Then, original dataset was altered by introducing artificial head motion. The generation of noisy data was done following the method exposed in<sup>10</sup> with values between  $-3$  and  $3$ . These dataset was preprocessed. Afterwards a second group of DMN was obtained applying a commonly used method for motion correction known as MCflirt,<sup>7</sup> it applies an optimized registration. Steps of registration, normalization, independent component analysis and DMN selection were also followed.

The third DMN group was obtained by using the altered and preprocessed dataset, applying an anisotropic filter as method for motion correction and applying the steps of registration, normalization, independent component analysis and DMN selection as was previously mentioned. The calculated tensor used as the basis for the anisotropic method was performed with the 3DAnisosmooth tool<sup>14,22,23,15</sup> and it is part of the software AFNI.<sup>24</sup> The filter is applied only one time, for this reason the iteration time parameter is set to only one iteration. The use of higher values of time iteration amplifies boundaries of smoothing and this produces loss of flow's information.

At the end three spatial DMN maps were obtained for each subject, these DMN were compared and analyzed with measurements of PSNR as is explain in next section.

#### 3.3 Performance Analysis

Performance of the motion correction method is tested using the groups of DMN detected and computing the measurement of peak signal noise ratio PSNR to compare the DMN obtained with different methods of motion correction.

PSNR was computed by using the DMN obtained from each subject but changing the motion correction methods. This is the baseline DMN image  $I_{ref}$  and the DMN obtained after applying to a noisy image a method for motion correction  $I_{test}$ .

The election of PSNR is because it estimates the quality of the reconstructed images with respect to an original image. So, it is a good measure for comparing restoration results for the same image. Here we are using the same image but adding noise to one and obtaining the independent component corresponding to the DMN. We are also sleuthing the connectivity by analyzing information's flow from internal neural structures represented in voxels with similar values of BOLD. Restored Images with higher PSNR are judged better.

#### 3.4 Results

The qualitative results correspond to spatial maps of the DMN that show the active areas corresponding to the IC most similar to the DMN template. The three DMN (baseline, and the ones from applying the anisotropic and state of art motion correction methods) are obtained from one of the subjects and are presented in Figure 2.

In these images, the DMN identified correspond to the areas associated to the DMN. An important restoration

of the mPFC is observed when the anisotropic method is applied. Region of PCC presents also good restoration of activation information after the anisotropic method. In axial slices can be observed that activation Bold signal in inferior parietal lobules apparently does not have a good restoration.

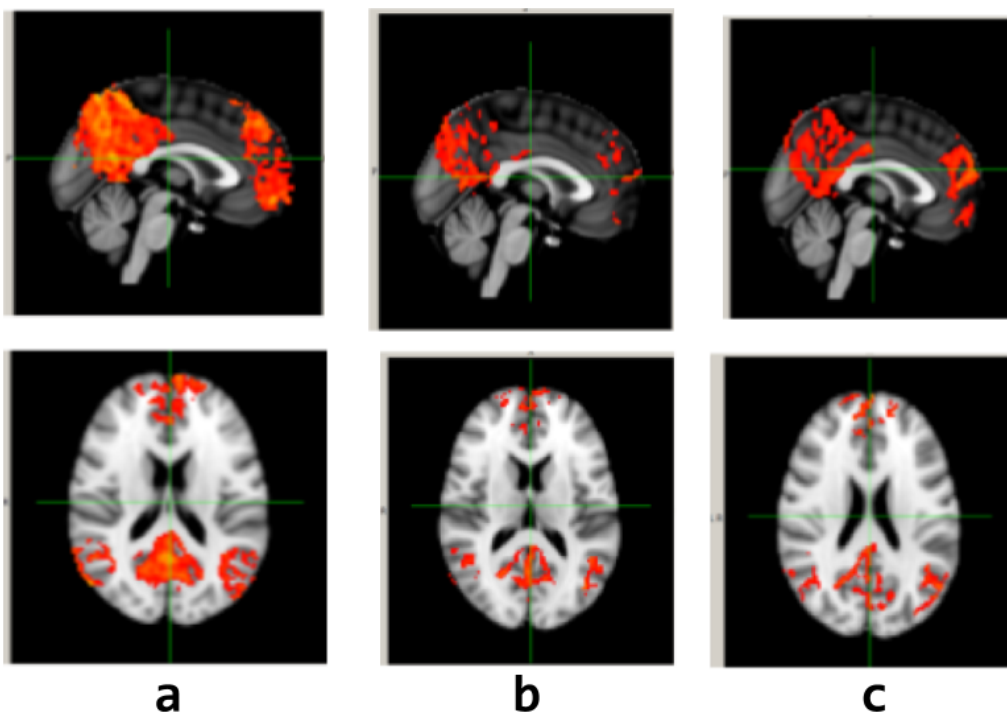


Figure 2: DMN obtained after the experimentation with data from a subject. The column **a** shows the sagittal and axial views of the DMN obtained as baseline. It is without noise and without apply any motion correction method. The column **b** belong to the sagittal and axial views of the DMN obtained after introducing artificial head movement and also applying the state of art method for motion correction (Mcflirt). The third column **c** belong to the DMN obtained after introduce artificial noise and applying the anisotropic approach for motion correction. A better detection of DMN is observed after applying the anisotropic method.

Quantitative results are presented in Figure 3. This picture shows the values of PSNR for DMN detected using the anisotropic method compared to the DMN detected after applying the state of art method of motion correction. Higher values of PSNR is good because it means that the ratio of Signal to Noise is higher. in the figure, PSNR values of DMN obtained with the anisotropic method are higher than the values of PSNR of the DMN obtained with the state of the art method. This is a evidence of how filtering in order to follow the information's flow can reduce the effect of head motion noise. Mean of the anisotropic results is higher for the dataset used for the experimentation as can be seen in Table 1. Additionally, as is presented in Table 2, the anisotropic method outperforms the state-of-the-art method by 5.93% PSNR.

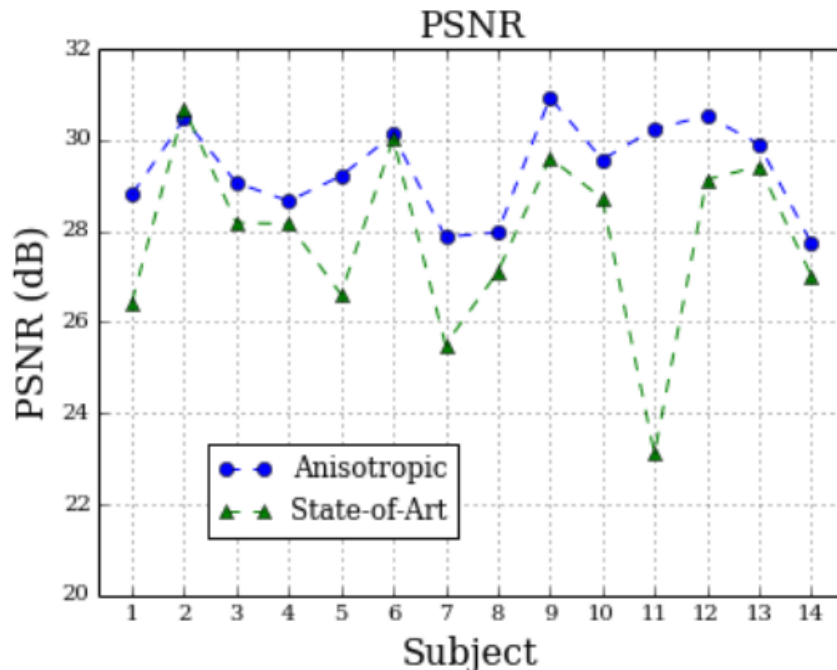


Figure 3: PSNR obtained for two groups of DMN, one obtained applying the anisotropic method for motion correction and the other group obtained applying the method of optimized registration of the state of the art.

Table 1: Mean of PSNR for the applied methods

	Mean Anisotropic	Mean state of art
PSNR	29.35	27.83

Table 2: Percentage of performance

Measurement	Percentage
PSNR	5.93

#### 4. DISCUSSION AND CONCLUSIONS

The aim of this study was to propose a method for motion correction based on anisotropic filtering of the functional data and compare the results of methods for motion correction and its utility for the detection of the DMN. Data from the performance of various methods for motion correction (like a standard method and the proposed one using anisotropic filter) are compared and results of the transformations performed are presented.

A method for enhance the detection of the DMN was proposed inspired on the organization of neural cells in the basal ganglia. The method was tested and compared the results with measurement of PSNR. The results show an improvement in the detection, less variability in the response of the DMN and a better detection by applying the anisotropic method. Results obtained show that the anisotropic approach outperforms the state-of-the-art method by 5.93% PSNR. The contribution presented is a model of how information is propagated and the use of this to improve the DMN restoration when some motion perturbs the network. This analysis is inspired by the fact that the nervous systems reduces dimensionality by structuring information hierarchically and anisotropically. This simple modification results to be very efficient in terms of recovery of the network perturbed by artifacts caused by head movement.

## ACKNOWLEDGMENTS

We are grateful to Norberto Malpica and Eva Manzanedo from IAIMBIO, Universidad Rey Juan Carlos III, Spain, who gave very friendly assistance taking and sharing the images from the 14 people used in this study.

## REFERENCES

- [1] Ogawa, S., Lee, T. M., Kay, A. R., and Tank, D. W., “Brain magnetic resonance imaging with contrast dependent on blood oxygenation.,” *Proceedings of the National Academy of Sciences of the United States of America* **87**(24), 9868–72 (1990).
- [2] Power, J. D., Mitra, A., Laumann, T. O., Snyder, A. Z., Schlaggar, B. L., and Petersen, S. E., “Methods to detect, characterize, and remove motion artifact in resting state fMRI,” *NeuroImage* **84**, 320–341 (2013).
- [3] Bruckner, R. Andrews, J. S. D., “The Brain’s Default Network,” **38**, 1–38 (2008).
- [4] Pardoe, H. R., Hiess, R. K., and Kuzniecky, R., “Motion and morphometry in clinical and nonclinical populations,” (2016).
- [5] Pujol, J., Macià, D., Blanco-Hinojo, L., Martínez-Vilavella, G., Sunyer, J., de la Torre, R., Caixàs, A., Martín-Santos, R., Deus, J., and Harrison, B. J., “Does motion-related brain functional connectivity reflect both artifacts and genuine neural activity?,” *NeuroImage* **101**, 87–95 (2014).
- [6] Power, J. D., Schlaggar, B. L., and Petersen, S. E., “Recent progress and outstanding issues in motion correction in resting state fMRI,” (2014).
- [7] Jenkinson, M., B. P. B. J. M. and Smith, S. M., “Improved optimisation for the robust and accurate linear registration and motion correction of brain images,” *NeuroImage* , 825–841 (2002).
- [8] Reimann, M. W., Nolte, M., Scolamiero, M., Turner, K., Perin, R., Chindemi, G., Dłotko, P., Levi, R., Hess, K., and Markram, H., “Cliques of neurons bound into cavities provide a missing link between structure and function,” *Frontiers in Computational Neuroscience* **11**, 48 (2017).
- [9] Charara, A., Sidibé, M., and Smith, Y., “Basal Ganglia Circuitry and Synaptic Connectivity,” *Surgical Treatment of Parkinson’s Disease and Other Movement Disorders* , 19–39 (2003).
- [10] Drobnyak, I., “Fmri simulator: Development and applications,” (2007).
- [11] Smith, S. M., “Fast robust automated brain extraction,” *Human brain mapping* **17**(3), 143–155 (2002).
- [12] Binnewijzend, M. A. A., Schoonheim, M. M., Wink, A. M., Flier, W. M. V. D., Tolboom, N., Adriaanse, S. M., Damoiseaux, J. S., Scheltens, P., Berckel, B. N. M. V., and Barkhof, F., “Resting-state fMRI changes in Alzheimer’s disease and mild cognitive impairment,” *NBA* **33**(9), 2018–2028 (2011).
- [13] Griffanti, L., Rolinski, M., Szewczyk-krolikowski, K., Menke, R. A., Filippini, N., Jenkinson, M., Hu, M. T. M., and Mackay, C. E., “Challenges in the reproducibility of clinical studies with resting state fMRI: An example in early Parkinson’s disease,” 1–13 (2016).
- [14] Weickert, J. and Schar, H., “A Scheme for Coherence-Enhancing Diffusion Filtering with Optimized Rotation Invariance,” (2000).
- [15] Ding, Z., Gore, J. C., and Anderson, A. W., “Reduction of noise in diffusion tensor images using anisotropic smoothing,” *Magnetic Resonance in Medicine* (2005).
- [16] Mazziotta, J. C., Toga, A. W., Evans, A., Fox, P., and Lancaster, J., “A probabilistic atlas of the human brain: Theory and rationale for its development: The international consortium for brain mapping (icbm),” *Neuroimage* **2**(2), 89–101 (1995).
- [17] Jenkinson, M. and Smith, S., “A global optimisation method for robust affine registration of brain images,” *Medical Image Analysis* , 5(2):143–156 (2001).
- [18] Baquero, K., Gómez, F., Cifuentes, C., Guldenmund, P., Demertzi, A., Vanhauzenhuyse, A., Gossier, O., Tshibanda, J.-F., Noirhomme, Q., Laureys, S., Soddu, A., and Romero, E., “A multiscale method for a robust detection of the default mode network,” (2013).
- [19] Liu, D., “Clustering analysis of default mode network in fmri data,” *IEEE* , 151–155 (2014).
- [20] Kelly, R. E., Alexopoulos, G. S., Wang, Z., Gunning, F. M., Murphy, C. F., Morimoto, S. S., Kanellopoulos, D., Jia, Z., Lim, K. O., and Hoptman, M. J., “Visual inspection of independent components: Defining a procedure for artifact removal from fmri data,” *Neuroscience Methods* **15**(1892), 233–245 (2010).

- [21] Wang, D., Kong, Y., Chu, W. C. W., Tam, C. W. C., Lam, L. C. W., Wang, Y., Northoff, G., Mok, V. C. T., Wang, Y., and Shi, L., "Generation of the probabilistic template of default mode network derived from resting-state fMRI," *IEEE Transactions on Biomedical Engineering* (2014).
- [22] Weickert, J., "Coherence-Enhancing Diffusion Filtering," *International Journal of Computer Vision* **31**(23), 111–127 (1999).
- [23] Gerig, G., Kubler, O., and Jolesz, F. A., "Nonlinear Anisotropic Filtering of MRI Data," **1**(2) (1992).
- [24] Cox, R., "Afni: Software for analysis and visualization of functional magnetic resonance neuroimages," 29:162–173 (1996).

# Bibliography

- [1] A. Charara, M. Sidibé, and Y. Smith, “Basal Ganglia Circuitry and Synaptic Connectivity,” *Surgical Treatment of Parkinson’s Disease and Other Movement Disorders*. Humana Press Inc., pp. 19–39, 2003.
- [2] F. L. Mastaglia and W. M. Carroll, “Evoked potentials in neurological diagnosis,” *British Medical Journal(Clinical research ed.)*, vol. 285, pp. 1678–1679, 1982.
- [3] B. Hans, “Über das Elektrenkephalogramm des Menschen,” *Archiv für Psychiatrie und Nervenkrankheiten*, pp. 87:527–570, 1929.
- [4] S. M. Smith, P. T. Fox, K. L. Miller, D. C. Glahn, P. M. Fox, C. E. Mackay, N. Filippini, K. E. Watkins, R. Toro, A. R. Laird, and C. F. Beckmann, “Correspondence of the brain’s functional architecture during activation and rest,” *Proceedings of the National Academy of Sciences of the United States of America*, vol. 106, pp. 13 040–13 045, 2009.
- [5] M. H. Lee, C. D. Smyser, and J. S. Shimony, “Resting State fMRI: A Review of Methods and Clinical Applications,” *AJNR. American journal of neuroradiology*, p. 1866–1872, 2013.
- [6] Y. I. Sheline and M. E. Raichle, “Resting State Functional Connectivity in Preclinical Alzheimer’s Disease,” *Biological Psychiatry*, vol. 74, no. 5, pp. 340–347, 2012.
- [7] J. S. D. Bruckner, R. Andrews, “The Brain’s Default Network: Anatomy, Function, and Relevance to Disease,” *Annals of the New York Academy of Sciences*, vol. 38, pp. 1–38, 2008.
- [8] A. Demertzi, F. Gómez, J. S. Crone, A. Vanhaudenhuyse, L. Tshibanda, Q. Noirhomme, M. Thonnard, V. Charland-Verville, M. Kirsch, S. Laureys, and A. Soddu, “Multiple fMRI system-level baseline connectivity is disrupted in patients with consciousness alterations,” *Cortex*, vol. 52, no. 1, pp. 35–46, 2014.
- [9] K. Baquero, F. Gómez, C. Cifuentes, P. Guldenmund, A. Demertzi, A. Vanhaudenhuyse, O. Gosseries, J.-F. Tshibanda, Q. Noirhomme, S. Laureys, A. Soddu, and E. Romero, “A multiscale method for a robust detection of the default mode network,” pp. 892 208–892 209, 2013.

- 
- [10] S.-g. Kim and K. Ugurbil, “Functional magnetic resonance imaging of the human brain,” *Journal of Neuroscience Methods*, vol. 74, pp. 229–243, 1997.
- [11] V. B. Mountcastle, “Modality and topographic properties of single neurons of cat’s somatic sensory cortex,” *Journal of Neurophysiology*, vol. 20, no. 4, pp. 408–434, 1957.
- [12] A. DG, *The anatomical organization of the central nervous system*. New York: McGraw-Hill 4th Edition ER Kandel, JH Schwartz, TM Jessell, Eds., 2000.
- [13] C. Roy and C. Sherrington, “On the Regulation of the Blood-Supply of the Brain,” *The Journal of physiology*, vol. 11, no. 1-2, pp. 85–158, 1890.
- [14] S. Ogawa, T. M. Lee, A. R. Kay, and D. W. Tank, “Brain magnetic resonance imaging with contrast dependent on blood oxygenation,” *Proceedings of the National Academy of Sciences of the United States of America*, vol. 87, no. 24, pp. 9868–72, 1990.
- [15] M. E. Raichle and A. Z. Snyder, “A default mode of brain function: A brief history of an evolving idea,” *NeuroImage*, vol. 2, no. 4, pp. 1083–1090, 2007.
- [16] J. D. Power, B. L. Schlaggar, and S. E. Petersen, “Recent progress and outstanding issues in motion correction in resting state fMRI,” *NeuroImage*, vol. 105, no. Supplement C, pp. 536 – 551, 2015.
- [17] *Brain Voyager Manual: Organizing, Processing and Analyzing fMRI data using Brain Voyager*, Institute for Imaging and Analytical Technologies, 2008. [Online]. Available: [http://www.i2at.msstate.edu/pdf/I2AT\\_Brain\\_Voyager\\_Manual\\_Rev11.19.pdf](http://www.i2at.msstate.edu/pdf/I2AT_Brain_Voyager_Manual_Rev11.19.pdf)
- [18] T. Krings, M. Reinges, S. Erberich, S. Kemeny, V. Rohde, U. Spetzger, M. Korinth, K. Willmes, J. Gilsbach, and A. Thron, “Functional MRI for presurgical planning problems, artifacts and solution strategies,” *Journal of Neurology Neuro Surgery and Psychiatry*, vol. 70, no. 6, pp. 749–760, 2001.
- [19] K. Friston, S. Williams, R. Howard, R. Frackowiak, and R. Turner, “Movement-Related effects in fMRI time-series,” *Magnetic Resonance in Medicine*, vol. 35, pp. 346 – 355, 1996.
- [20] J. D. Power, A. Mitra, T. O. Laumann, A. Z. Snyder, B. L. Schlaggar, and S. E. Petersen, “Methods to detect, characterize, and remove motion artifact in resting state fMRI,” *NeuroImage*, vol. 84, pp. 320–341, 2013.
- [21] A. X. Patel, P. Kundu, M. Rubinov, P. S. Jones, P. E. Vértes, K. D. Ersche, J. Suckling, and E. T. Bullmore, “A wavelet method for modeling and despiking motion artifacts from resting-state fMRI time series,” *NeuroImage*, vol. 95, pp. 287–304, 2014.

- [22] R. Kelly, G. Alexopoulos, Z. Wang, F. Gunning-Dixon, C. Murphy, S. Morimoto, T. Kanellopoulos, Z. Jia, K. O Lim, and M. Hoptman, “Visual inspection of independent components: Defining a procedure for artifact removal from fMRI data,” *Journal of Neuroscience Methods*, vol. 189, pp. 233–45, 04 2010.
- [23] L. Griffanti, G. Salimi-Khorshidi, C. F. Beckmann, E. J. Auerbach, G. Douaud, C. E. Sexton, E. Zsoldos, K. P. Ebmeier, N. Filippini, C. E. Mackay, S. Moeller, J. Xu, E. Yacoub, G. Baselli, K. Ugurbil, K. L. Miller, and S. M. Smith, “ICA-based artefact removal and accelerated fMRI acquisition for improved resting state network imaging,” *NeuroImage*, vol. 95, pp. 232–247, 2014.
- [24] H. R. Pardoe, R. K. Hiess, and R. Kuzniecky, “Motion and morphometry in clinical and non clinical populations,” *NeuroImage*, vol. 135, no. Supplement C, pp. 177 – 185, 2016.
- [25] J. Pujol, D. Macià, L. Blanco-Hinojo, G. Martínez-Vilavella, J. Sunyer, R. de la Torre, A. Caixàs, R. Martín-Santos, J. Deus, and B. J. Harrison, “Does motion-related brain functional connectivity reflect both artifacts and genuine neural activity?” *NeuroImage*, vol. 101, pp. 87–95, 2014.
- [26] N. J. Herrero M.T, Barcia C, “Functional anatomy of thalamus and basal ganglia,” *Child’s Nervous System*, vol. 18, p. 386–404, 2002.
- [27] H. A. Riley, *An atlas of the Basal ganglia brain stem and spinal cord based on Myelin stained material*. New York: Hafner, 1960.
- [28] D. Greene, T. Laumann, J. Dubis, S. Ihnen, M. Neta, J. Power, J. Pruett, K. Black, and B. Schlaggar, “Developmental changes in the organization of functional connections between the basal ganglia and cerebral cortex,” *Journal of Neuroscience*, vol. 34, no. 17, pp. 5842–5854, 2014.
- [29] A. Nambu, “A new dynamic model of the cortico-basal ganglia loop,” in *Brain Mechanisms for the Integration of Posture and Movement*, ser. Progress in Brain Research. Elsevier, 2004, vol. 143, no. Supplement C, pp. 461 – 466.
- [30] J. Park, “Movement Disorders Following Cerebrovascular Lesion in the Basal Ganglia Circuit,” *JMD, Journal of movement disorder*, pp. 71–79, 2016.
- [31] G. Chevalier and J.-M. M. Deniau, “Disinhibition as a basic process in the expression of striatal functions II. The striato-nigral influence on thalamocortical cells of the ventromedial thalamic nucleus,” *Brain Research*, vol. 334, no. 2, pp. 227 – 233, 1985.
- [32] P. Perona and J. Malik, “Scale-Space and Edge Detection Using Anisotropic Diffusion,” *IEEE Transactions on pattern analysis and machine intelligence*, vol. 12, no. 7, 1990.

- 
- [33] J. Weickert, *Anisotropic Diffusion in Image Processing*. Stuttgart: B. G. Teubner, 1998.
- [34] U. Weickert, “Coherence-Enhancing Diffusion Filtering,” *International Journal of Computer Vision*, vol. 31, no. 23, pp. 111–127, 1999.
- [35] J. Weickert and H. Schar, “A Scheme for Coherence-Enhancing Diffusion Filtering with Optimized Rotation Invariance,” *Journal of Visual Communication and Image Representation*, vol. 13, no. 1, pp. 103 – 118, 2002.
- [36] G. Gerig, O. Kubler, and F. A. Jolesz, “Nonlinear anisotropic filtering of MRI data,” *IEEE Transactions on Medical Imaging*, vol. 11, no. 2, 1992.
- [37] Z. Ding, J. C. Gore, and A. W. Anderson, “Reduction of noise in diffusion tensor images using anisotropic smoothing,” *Magnetic Resonance in Medicine*, vol. 53, no. 2, pp. 485–490, 2005.
- [38] X.-n. Zuo and X.-x. Xing, “Effects of Non-Local Diffusion on Structural MRI Preprocessing and Default Network Mapping: Statistical Comparisons with Isotropic/Anisotropic Diffusion,” *PLOS ONE*, vol. 6, no. 10, pp. 1–9, 2011.
- [39] I. Drobnjak, “Mri simulator: Development and applications,” Ph.D. dissertation, University of Oxford, 2007.
- [40] S. M. Smith, “Fast robust automated brain extraction,” *Human brain mapping*, vol. 17, no. 3, pp. 143–155, 2002.
- [41] M. A. Binnewijzend, M. M. Schoonheim, E. Sanz-Arigita, A. M. Wink, W. M. van der Flier, N. Tolboom, S. M. Adriaanse, J. S. Damoiseaux, P. Scheltens, B. N. van Berckel, and F. Barkhof, “Resting-state fMRI changes in Alzheimer’s disease and mild cognitive impairment,” *NBA*, vol. 33, no. 9, pp. 2018–2028, 2011.
- [42] L. Griffanti, “Effective artifact removal in resting state fMRI data improves detection of DMN functional connectivity alteration in Alzheimer’s disease,” *Frontiers in Human Neuroscience*, vol. 9, no. August, pp. 1–11, 2015.
- [43] J. C. Mazziotta, A. W. Toga, A. Evans, P. Fox, and J. Lancaster, “A probabilistic atlas of the human brain: Theory and rationale for its development: The international consortium for brain mapping (icbm),” *Neuroimage*, vol. 2, no. 2, pp. 89–101, 1995.
- [44] M. Jenkinson, P. Bannister, J. M. Brady, and S. M. Smith, “Improved Optimisation for the Robust and Accurate Linear Registration and Motion Correction of Brain Images,” *NeuroImage*, pp. 825–841, 2002.

- 
- [45] M. Jenkinson and S. Smith, “A global optimisation method for robust affine registration of brain images,” *Medical Image Analysis*, pp. 5(2):143–156, 2001.
  - [46] D. Liu, “Clustering analysis of default mode network in fMRI data,” *IEEE*, pp. 151–155, 2014.
  - [47] C. F. Beckmann and S. M. Smith, “Probabilistic independent component analysis for functional magnetic resonance imaging,” *IEEE Transactions on Medical Imaging*, vol. 23, no. 2, pp. 137–152, Feb 2004.
  - [48] D. Wang, Y. Kong, W. C. W. Chu, C. W. C. Tam, L. C. W. Lam, Y. Wang, G. Northoff, V. C. T. Mok, Y. Wang, and L. Shi, “Generation of the probabilistic template of default mode network derived from resting-state fMRI,” *IEEE Transactions on Biomedical Engineering*, 2014.